J. Fluid Mech. (2018), vol. 849, pp. 111–135.
doi:10.1017/jfm.2018.422

On the steady-state resonant acoustic–gravity waves

Xiaoyan Yang[3], Frederic Dias[4] and Shijun Liao[1,2,3,†]

[1]State Key Laboratory of Ocean Engineering, Shanghai 200240, PR China

[2]Collaborative Innovative Center for Advanced Ship and Deep-Sea Exploration, Shanghai 200240, PR China

[3]School of Naval Architecture, Ocean and Civil Engineering, Shanghai Jiao Tong University, Shanghai 200240, PR China

[4]School of Mathematics and Statistics, University College Dublin, MaREI Centre, Belfield Dublin 4, Ireland

(Received 20 January 2018; revised 15 May 2018; accepted 17 May 2018)

The steady-state interaction of acoustic–gravity waves in an ocean of uniform depth is researched theoretically by means of the homotopy analysis method (HAM), an analytic approximation method for nonlinear problems. Considering compressibility, a hydroacoustic wave can be produced by the interaction of two progressive gravity waves with the same wavelength travelling in opposite directions, which contains an infinite number of small denominators in the framework of the classical analytic approximation methods, like perturbation methods. Using the HAM, the infinite number of small denominators are avoided once and for all by means of choosing a proper auxiliary linear operator. Besides, by choosing a proper 'convergence-control parameter', convergent series solutions of the steady-state acoustic–gravity waves are obtained in cases of both non-resonance and exact resonance. It is found, for the first time, that the steady-state resonant acoustic–gravity waves widely exist. In addition, the two primary wave components and the resonant hydroacoustic wave component might occupy most of wave energy. It is found that the dynamic pressure on the sea bottom caused by the resonant hydroacoustic wave component is much larger than that in the case of non-resonance, which might even trigger microseisms of the ocean floor. All of these might deepen our understanding and enrich our knowledge of acoustic–gravity waves.

Key words: surface gravity waves, waves/free-surface flows

1. Introduction

The first theoretical work on hydroacoustic waves was done by Longuet-Higgins (1950), who argued that the water can be treated as incompressible only when the time taken for the disturbance to propagate to the bottom is small compared to the period of waves. Considering the compressibility of water, Longuet-Higgins (1950) found that hydroacoustic waves, which affect the whole water column, can be

† Email address for correspondence: sjliao@sjtu.edu.cn

generated by the nonlinear interaction of two progressive gravity waves with the same wavelength travelling in opposite directions. Longuet-Higgins (1950) also mentioned that the resonant triad interactions of acoustic–gravity waves exist at the special water depths $h \approx (n+0.5)\pi c/\omega_3$, where $n = 0, 1, 2, \ldots$, h is the water depth, c is the speed of sound in the water, which is of the order of 1500 m s^{-1} and ω_3 is the frequency of the resulting hydroacoustic wave. However, Longuet-Higgins (1950) did not obtain solutions of resonant acoustic–gravity waves. Later, Kibblewhite & Wu (1991) argued that the hydroacoustic wave can be generated by two opposite gravity waves with slightly different wavenumbers. The interaction between two primary gravity waves and the resulting hydroacoustic wave can be described as

$$\boldsymbol{k}_1 + \boldsymbol{k}_2 = \boldsymbol{k}_3, \quad \omega_1 + \omega_2 = \omega_3, \quad 0 \leqslant |\boldsymbol{k}_3| < \omega_3/c, \tag{1.1a–c}$$

unskip where $\boldsymbol{k}_1$, $\boldsymbol{k}_2$ and ω_1, ω_2 are the wavenumbers and wave frequencies of two primary gravity waves, $\boldsymbol{k}_3$ is the horizontal component of the wavenumber of the hydroacoustic wave. For the Longuet-Higgins case, $|\boldsymbol{k}_3|$ is equal to 0. When $|\boldsymbol{k}_3| \geqslant \omega_3/c$, the hydroacoustic response degenerates into an inhomogeneous wave decaying with increasing water depth. In this paper, we consider the non-resonance and resonance cases of Longuet-Higgins with $|\boldsymbol{k}_3| = 0$ and one more general resonance case with $0 < |\boldsymbol{k}_3| < \omega_3/c$. The interactions of two gravity waves travelling in opposite directions were investigated by many researchers, such as Kibblewhite & Ewans (1985), Webb (1992, 1998), Bowen *et al.* (2003), Naugolnikh & Rybak (2003), Farrell & Munk (2010), Ardhuin & Herbers (2013), Ardhuin *et al.* (2013). But none of them focussed on the exact resonance of waves.

Recently, considering the resonance of two opposite gravity waves and the resulting hydroacoustic wave, Kadri & Stiassnie (2013) found that the condition for the exactly resonating triads is

$$\omega_3^2 = g\lambda_3 \tanh(\lambda_3 h), \tag{1.2}$$

where g is the gravitational acceleration, λ_3 is a parameter associated with the vertical wavenumber of the hydroacoustic wave. They found that when the resonance condition is satisfied, the amplitude equations of the resonant acoustic–gravity triads are the same as those of resonant gravity triads (Phillips 1960; Benney 1962; Longuet-Higgins 1962; Bretherton 1964). This conclusion was confirmed by Kadri & Akylas (2016), who obtained resonant acoustic–gravity waves with periodically changing wave spectrum and found that the interaction time scale is longer than that of a standard resonant triad. Note that, without considering the compressibility of the water, three-wave resonance does not occur for gravity waves (Dyachenko & Zakharov 1994). Kadri (2015) followed Longuet-Higgins (1950) to generalize the resonance condition of the acoustic–gravity waves and found that the resonances given by Longuet-Higgins (1950) are just particular cases. Kadri (2015) also got the solution of the Longuet-Higgins resonance case, which is similar to that obtained by Kadri & Stiassnie (2013). However, to the best of our knowledge, the steady-state resonant acoustic–gravity waves with time-independent wave spectrum have never been obtained before in water of uniform depth.

On the other hand, the studies of two progressive gravity waves in opposite directions focused on the pressure field of the water, especially on the bottom. Even without considering the compressibility of the water, the interaction can produce a second-order pressure term that does not attenuate with depth. In particular, Renzi & Dias (2014) mentioned that the compressibility is not the main driving mechanism. This conclusion was confirmed by Pellet *et al.* (2017) who obtained a second-order pressure field generated by two opposite travelling gravity waves, which is independent of water depth and periodic in time with twice the frequency of the primary gravity waves. Besides, considering the compressibility of the water, Longuet-Higgins (1950) and Kadri & Stiassnie (2013) obtained the solution of acoustic–gravity waves in the case of non-resonance. Kadri & Stiassnie (2013) and Kadri & Akylas (2016) got the solution of exact resonance acoustic–gravity waves with periodic wave spectrum. So, the pressure on the bottom of the water, which is dependent of water depth and time, can be obtained directly. In addition, the hydroacoustic waves produced by a moving bottom were studied by Yamamoto (1982), Stiassnie (2010), Oliveira & Kadri (2016) and Kadri (2017). Eyov *et al.* (2013) and Kadri & Stiassnie (2012) studied effects of different hydroacoustic modes on two types of bottoms (an elastic bottom and a bottom with a step) in a compressible ocean. Note that these studies related to the motion of the bottom did not consider the exact resonance.

In this paper, we first consider the non-resonance conditions of acoustic–gravity waves, the solutions of which have been obtained previously, for example by Longuet-Higgins (1950) and Kadri & Stiassnie (2013). But, more importantly, we focus on the steady-state resonant triad interactions of acoustic–gravity waves with time-independent wave spectrum, which have never been obtained before. We use the resonance condition

$$\omega_3^2 = g(\lambda_3^2 - \gamma^2)/[\lambda_3 \coth(\lambda_3 h) - \gamma], \tag{1.3}$$

where $\gamma = g/2c^2$, which is similar to (1.2) given by Kadri & Stiassnie (2013), who found that all amplitudes of the wave components vary periodically, i.e. with periodic wave spectrum, when the resonance condition is exactly satisfied. Are there any steady-state resonant acoustic–gravity waves whose spectrum is independent of time? In this steady-state system, there is no exchange of wave energy between different wave components, i.e. all amplitudes of wave components are independent of time. For the normal gravity waves, the answer is yes. Liao (2011*b*) found steady-state resonant gravity waves in deep water by means of the homotopy analysis method (HAM) (Liao 1992, 2003, 2010, 2011*a*; Van Gorder & Vajravelu 2008; Vajravelu & Van Gorder 2012; Zhong & Liao 2017, 2018*a*,*b*). Then it was found that the steady-state resonant gravity waves exist extensively in both infinite and finite water depth by Xu *et al.* (2012) and Liu & Liao (2014), which were even confirmed experimentally by Liu *et al.* (2015). In addition, Liao, Xu & Stiassnie (2016) successfully applied the HAM to obtain the steady-state nearly resonant gravity waves in deep water, and Liu, Xu & Liao (2018) found finite amplitude steady-state waves with multiple near-resonant interactions. The purpose of this paper is to confirm the existence of the steady-state resonant acoustic–gravity waves.

It has been commonly accepted that the generation of hydroacoustic waves in the ocean is due to the nonlinear interaction of two gravity waves that travel in opposite directions. If we ignore the compressibility of water, two gravity waves travelling in opposite directions with the same amplitude and wavelength create a standing wave with an infinite number of 'singularities' (i.e. zero denominators) when one uses classical methods, like perturbation methods. As mentioned by Dias & Bridges (2006), most studies of standing waves are based on semi-analytical methods and numerical methods because of the inherent analytical difficulties. So, the first obstacle of acoustic–gravity waves in deep water is how to handle the small denominators which are similar to the 'singularities' in the problem of standing waves, which is a big challenge in the framework of perturbation methods, as mentioned by Madsen & Fuhrman (2012). Besides, when the exact resonance condition is satisfied, one more 'singularity' corresponding to the hydroacoustic wave component must be considered.

In this paper, the acoustic–gravity wave problem is solved by means of the homotopy analysis method (HAM), an analytic technique for nonlinear problems. Using the HAM, the infinite number of small denominators in the acoustic–gravity waves problem can be avoided conveniently once and for all by means of choosing a proper auxiliary linear operator, as described later in this paper. Besides, different from perturbation methods, the HAM has nothing to do with any small/large physical parameters. More importantly, it provides us a simple way to guarantee the convergence of the solution.

The structure of the paper is presented below. The mathematical formulae are described in § 2. The solutions of non-resonant acoustic–gravity waves are given in § 3.1. The steady-state resonant triad interactions of acoustic–gravity waves are studied in detail in § 3.2. Conclusions and discussions are presented in § 4.

2. Mathematical formulae

2.1. *Governing equations*

Let us consider the nonlinear interactions of two progressive gravity waves and one hydroacoustic wave in water of uniform depth. A Cartesian coordinate system is adopted with the x-axis and the y-axis located on the mean water plane and the z-axis pointing vertically upwards. Longuet-Higgins (1950) derived the water wave equations together with their boundary conditions in a heavy compressible fluid, in the absence of viscosity and surface tension. The governing equation for the velocity potential has linear, quadratic and cubic terms. Kadri & Stiassnie (2013) used the same governing equation as Longuet-Higgins, without the cubic term. Here we use the same equation as Longuet-Higgins without the nonlinear terms. The justification is given in the paper by Longuet-Higgins (1950) itself. Indeed, Longuet-Higgins solved for the velocity potential by using a method of successive approximations. At second order, the velocity potential given by his equation (159) has five types of terms. Longuet-Higgins writes below his equation (169) that the first two terms in equation (159) are negligible compared with the fourth, and then writes a simplified expression for the second-order velocity potential (see his equation (172)). We checked that this is equivalent to neglecting the quadratic terms in the governing equation. Therefore, in our paper, we use the governing equation

$$\frac{\partial^2\varphi}{\partial t^2} - c^2\nabla^2\varphi + g\frac{\partial\varphi}{\partial z} = 0, \quad -h \leqslant z \leqslant \eta(x, y, t), \ (x, y) \in \mathbb{R}^2, \tag{2.1}$$

subject to the boundary conditions:

$$\frac{\partial^2\varphi}{\partial t^2} + g\frac{\partial\varphi}{\partial z} + \frac{\partial|\nabla\varphi|^2}{\partial t} + \nabla\varphi\cdot\nabla\left(\frac{1}{2}|\nabla\varphi|^2\right) = 0, \quad \text{on } z = \eta(x, y, t), \tag{2.2}$$

$$g\eta + \frac{\partial\varphi}{\partial t} + \frac{1}{2}|\nabla\varphi|^2 = 0, \quad \text{on } z = \eta(x, y, t), \tag{2.3}$$

$$\lim_{z\to -h}\frac{\partial\varphi}{\partial z} = 0, \tag{2.4}$$

where

$$\nabla = \boldsymbol{i}\frac{\partial}{\partial x} + \boldsymbol{j}\frac{\partial}{\partial y} + \boldsymbol{k}\frac{\partial}{\partial z} \tag{2.5}$$

is a linear operator with $\boldsymbol{i}, \boldsymbol{j}, \boldsymbol{k}$ denoting the unit vector in the x, y, z direction, φ is the velocity potential, η is the wave elevation, t denotes the time, h is the water depth, c is the speed of sound in water, g is the acceleration due to gravity, respectively. Note that the governing equation (2.1) was also used by Kadri & Stiassnie (2013). The pressure field of the water can be obtained by Bernoulli's equation

$$\begin{aligned} p &= p_a - \rho g z - \rho\left(\frac{\partial \varphi}{\partial t} + \frac{1}{2}\frac{\partial \varphi^2}{\partial x} + \frac{1}{2}\frac{\partial \varphi^2}{\partial y} + \frac{1}{2}\frac{\partial \varphi^2}{\partial z}\right) \\ &= p_a - \rho g z + p_d, \quad -h \leqslant z \leqslant \eta(x, y, t), \quad (x, y) \in \mathbb{R}^2, \end{aligned} \tag{2.6}$$

where $p_a - \rho g z$ is the hydrostatic pressure and p_d is the dynamic pressure, $\rho = 1025\ \mathrm{kg\ m^{-3}}$.

The linear solutions of the governing equations (2.1)–(2.4) given by Dalrymple & Rogers (2006) read

$$\varphi = \frac{g\mathrm{i}\tilde{A}}{2\omega}\frac{\lambda\cosh[\lambda(h+z)] - \gamma\sinh[\lambda(h+z)]}{\lambda\cosh(\lambda h) - \gamma\sinh(\lambda h)}\mathrm{e}^{\gamma z}\mathrm{e}^{\mathrm{i}(\boldsymbol{k}\cdot\boldsymbol{r} - \omega t)}, \tag{2.7}$$

where $\gamma = g/2c^2$, $k^2 = \lambda^2 + \omega^2/c^2 - \gamma^2$ and the dispersion relation is given by

$$\omega^2 = g(\lambda^2 - \gamma^2)/[\lambda\coth(\lambda h) - \gamma], \tag{2.8}$$

where $\tilde{A}$ denotes the wave amplitude, $\boldsymbol{k}$ is the wavenumber, $k = |\boldsymbol{k}|$, ω is the wave frequency and $\boldsymbol{r} = x\boldsymbol{i} + y\boldsymbol{j}$.

Let σ_i denote the actual wave frequency of two primary gravity waves. Due to the weakly nonlinearity on the free surface of the water, the actual wave frequency σ_i is slightly different from the linear frequency ω_i. Write

$$\epsilon_i = \frac{\sigma_i}{\omega_i}, \quad i = 1, 2, \tag{2.9}$$

where the value of ϵ_i is slightly different from 1. Then, we define the variables

$$\xi_i = \boldsymbol{k}_i \cdot \boldsymbol{r} - \sigma_i t, \quad i = 1, 2. \tag{2.10}$$

For steady-state wave systems, all wave amplitudes a_i, wavenumbers $\boldsymbol{k}_i$ and actual wave frequencies σ_i, where $i = 1, 2$, are time independent. Using the new variables ξ_i, the original initial/boundary-value problem governed by (2.1)–(2.4) can be transformed into a boundary-value one. In the new coordinate system (ξ_1, ξ_2, z), the governing equation (2.1) becomes

$$\begin{aligned} &\sum_{i=1}^{2}\sum_{j=1}^{2}\sigma_i\sigma_j\frac{\partial^2\varphi}{\partial\xi_i\xi_j} - c^2\sum_{i=1}^{2}\sum_{j=1}^{2}\boldsymbol{k}_i\cdot\boldsymbol{k}_j\frac{\partial^2\varphi}{\partial\xi_i\xi_j} \\ &\quad - c^2\frac{\partial^2\varphi}{\partial z^2} + g\frac{\partial\varphi}{\partial z} = 0, \quad -h \leqslant z \leqslant \eta(\xi_1, \xi_2), \end{aligned} \tag{2.11}$$

subject to the two boundary conditions on the unknown free surface $z=\eta(\xi_1,\xi_2)$,

$$\begin{aligned}\mathcal{N}_1[\varphi,\sigma_1,\sigma_2] &= \sum_{i=1}^{2}\sum_{j=1}^{2}\sigma_i\sigma_j\frac{\partial^2\varphi}{\partial\xi_i\xi_j}+g\frac{\partial\varphi}{\partial z}-2\sum_{i=1}^{2}\sigma_i\frac{\partial f}{\partial\xi_i}\\ &\quad+\sum_{i=1}^{2}\sum_{j=1}^{2}\boldsymbol{k}_i\boldsymbol{\cdot}\boldsymbol{k}_j\frac{\partial\varphi}{\partial\xi_i}\frac{\partial f}{\partial\xi_j}+\frac{\partial\varphi}{\partial z}\frac{\partial f}{\partial z}=0,\quad \text{on } z=\eta(\xi_1,\xi_2),\end{aligned} \tag{2.12}$$

$$\mathcal{N}_2[\varphi,\eta,\sigma_1,\sigma_2]=\eta-\frac{1}{g}\left(\sum_{i=1}^{2}\sigma_i\frac{\partial\varphi}{\partial\xi_i}-f\right)=0,\quad \text{on } z=\eta(\xi_1,\xi_2), \tag{2.13}$$

and one impermeable condition at the bottom,

$$\lim_{z\to -h}\frac{\partial\varphi}{\partial z}=0, \tag{2.14}$$

where

$$f=\frac{1}{2}\left[\sum_{i=1}^{2}\sum_{j=1}^{2}\boldsymbol{k}_i\boldsymbol{\cdot}\boldsymbol{k}_j\frac{\partial\varphi}{\partial\xi_i}\frac{\partial\varphi}{\partial\xi_j}+\left(\frac{\partial\varphi}{\partial z}\right)^2\right] \tag{2.15}$$

and $\mathcal{N}_1$ and $\mathcal{N}_2$ are two nonlinear operators defined above.

For a steady-state wave system, there is no exchange of wave energy between different wave components, i.e. all physical quantities related to the wave systems are constant. Thus, the steady-state wave elevation $\eta(\xi_1,\xi_2)$ can be expressed by

$$\eta(\xi_1,\xi_2)=\sum_{m_1=0}^{+\infty}\sum_{m_2=-\infty}^{+\infty}a_{m_1,m_2}\cos(m_1\xi_1+m_2\xi_2), \tag{2.16}$$

where a_{m_1,m_2} is a constant to be determined later. Similarly, according to the governing equations (2.11) and the bottom boundary condition (2.14), the velocity potential $\varphi(\xi_1,\xi_2,z)$ should be in the form

$$\varphi(\xi_1,\xi_2,z)=\sum_{m_1=0}^{+\infty}\sum_{m_2=-\infty}^{+\infty}b_{m_1,m_2}\Psi_{m_1,m_2}(\xi_1,\xi_2,z), \tag{2.17}$$

with the definition

$$\begin{aligned}\Psi_{m_1,m_2}(\xi_1,\xi_2,z) &= \frac{\lambda_{m_1,m_2}\cosh[\lambda_{m_1,m_2}(h+z)]-\gamma\sinh[\lambda_{m_1,m_2}(h+z)]}{\lambda_{m_1,m_2}\cosh(\lambda_{m_1,m_2}h)-\gamma\sinh(\lambda_{m_1,m_2}h)}\\ &\quad\times \mathrm{e}^{\gamma z}\sin(m_1\xi_1+m_2\xi_2),\end{aligned} \tag{2.18}$$

where b_{m_1,m_2} is a constant to be determined later. It should be emphasized that (2.17) automatically satisfies the bottom boundary condition (2.14). It also satisfies the governing equation (2.11), provided that $k^2_{m_1,m_2}=\lambda^2_{m_1,m_2}+\sigma^2_{m_1,m_2}/c^2-\gamma^2$, where $k_{m_1,m_2}=|m_1\boldsymbol{k}_1+m_2\boldsymbol{k}_2|$, $\sigma_{m_1,m_2}=m_1\sigma_1+m_2\sigma_2$. Because the nonlinearities in the paper of all examples are weak, we choose $\lambda^2_{m_1,m_2}\approx k^2_{m_1,m_2}-\omega^2_{m_1,m_2}/c^2+\gamma^2$, where $\omega_{m_1,m_2}=m_1\omega_1+m_2\omega_2$. The corresponding parameter λ in (2.7) is λ_{m_1,m_2}. Thus, the unknown coefficients a_{m_1,m_2} and b_{m_1,m_2} are determined by the two fully nonlinear boundary conditions (2.12) and (2.13). Once the velocity potential is obtained, we can directly obtain the pressure field of the water from (2.6). Here, we focus on the dynamic pressure p_d in the whole water field. From (2.17), the dynamic pressure p_d is in the form as

$$p_d(\xi_1, \xi_2, z) = \rho \sum_{m_1=0}^{+\infty} \sum_{m_2=-\infty}^{+\infty} \left(\omega^2_{m_1,m_2} + \frac{1}{2} k^2_{m_1,m_2} - \frac{1}{2} \lambda^2_{m_1,m_2} \right) b_{m_1,m_2} \Psi_{m_1,m_2}. \tag{2.19}$$

Based on (1.1*a–c*), we consider the case $k_1 = |\boldsymbol{k}_1|$ slightly different from $k_2 = |\boldsymbol{k}_2|$. When $m_1 \neq m_2$, the value of $(\omega^2_{m_1,m_2}/c^2 - \gamma^2)$ is very small (the frequency ω_i of the primary waves considered in this paper is around 1 s^{-1}) compared to k_{m_1,m_2}, so that $\lambda_{m_1,m_2} \approx k_{m_1,m_2}$, which represents gravity waves in water of uniform depth. When $m_1 = m_2$, k_{m_1,m_2} is very small. λ_{m_1,m_2} is an imaginary number, which represents the hydroacoustic wave. Further, when $m_1 = m_2 > 1$, the corresponding hydroacoustic wave is generated by two high-order gravity waves. In this paper, we focus on the resulting hydroacoustic wave, when $m_1 = m_2 = 1$.

2.2. *Solution procedure*

In 2011, Liao (2011*b*) successfully applied the HAM to obtain the solutions of steady-state resonant gravity waves governed by the fully nonlinear wave equations. Thereafter, Xu *et al.* (2012), Liu & Liao (2014), Liao *et al.* (2016) and Liu *et al.* (2018) made further contributions in the study of steady-state resonant gravity waves. Detailed mathematical derivations can be found in these articles. So, for the sake of simplicity, we just give some important formulae here.

Let $q \in [0, 1]$ denote an embedding parameter. In the framework of HAM, we first construct a family of solutions $\Phi(\xi_1, \xi_2, z; q)$, $\zeta(\xi_1, \xi_2; q)$, $\Lambda_1(q)$ and $\Lambda_2(q)$ in $q \in [0, 1]$ by means of the so-called zeroth-order deformation equations,

$$\sum_{i=1}^{2} \sum_{j=1}^{2} \sigma_i \sigma_j \frac{\partial^2 \Phi}{\partial \xi_i \xi_j} - c^2 \sum_{i=1}^{2} \sum_{j=1}^{2} \boldsymbol{k}_i \cdot \boldsymbol{k}_j \frac{\partial^2 \Phi}{\partial \xi_i \xi_j} - c^2 \frac{\partial^2 \Phi}{\partial z^2} + g \frac{\partial \Phi}{\partial z} = 0, \quad -h \leqslant z \leqslant \zeta(\xi_1, \xi_2; q), \tag{2.20}$$

subject to the two boundary conditions on the unknown wave elevation $z = \eta(\xi_1, \xi_2; q)$

$$(1-q)\mathcal{L}^*[\Phi(\xi_1, \xi_2, z; q) - \varphi_0(\xi_1, \xi_2, z)] = c_0 q \mathcal{N}_1[\Phi(\xi_1, \xi_2, z; q), \Lambda_1(q), \Lambda_2(q)], \tag{2.21}$$

$$(1-q)\zeta(\xi_1, \xi_2; q) = c_0 q \mathcal{N}_2[\Phi(\xi_1, \xi_2, z; q), \zeta(\xi_1, \xi_2; q), \Lambda_1(q), \Lambda_2(q)], \tag{2.22}$$

and the impermeable condition at the bottom

$$\lim_{z \to -h} \frac{\partial \Phi}{\partial z} = 0, \tag{2.23}$$

where $\mathcal{N}_1$ and $\mathcal{N}_2$ are the two nonlinear operators defined by (2.12) and (2.13), $\mathcal{L}^*$ is an auxiliary linear operator and $\varphi_0(\xi_1, \xi_2, z)$ is an initial guess of $\varphi(\xi_1, \xi_2, z)$, $c_0 \neq 0$ is the so-called 'convergence-control parameter' without physical meaning, respectively. Here, Φ, ζ, Λ_1, Λ_2 correspond to the unknown φ, η, σ_1, σ_2, respectively. It should be emphasized that we have great freedom to choose the auxiliary linear operator. Obviously, when $q=0$,

$$\Phi(\xi_1, \xi_2, z; 0) = \varphi_0(\xi_1, \xi_2, z), \quad \zeta(\xi_1, \xi_2; 0) = 0. \tag{2.24a,b}$$

When $q=1$, equations (2.20)–(2.23) are equivalent to the original equations (2.11)–(2.14), respectively, therefore we have

$$\Phi(\xi_1, \xi_2, z; 1) = \varphi(\xi_1, \xi_2, z), \quad \zeta(\xi_1, \xi_2; 1) = \eta(\xi_1, \xi_2), \quad \Lambda_1(1) = \sigma_1, \quad \Lambda_2(1) = \sigma_2. \tag{2.25a–d}$$

Thus, as q increases from 0 to 1, $\Phi(\xi_1, \xi_2, z; q)$ deforms continuously from the initial guess $\varphi_0(\xi_1, \xi_2, z)$ to the unknown potential function $\varphi(\xi_1, \xi_2, z)$, so does $\zeta(\xi_1, \xi_2; q)$ from 0 to the unknown wave profile $\eta(\xi_1, \xi_2)$, $\Lambda_1(q)$, $\Lambda_2(q)$ from the initial guesses $\sigma_{1,0}$, $\sigma_{2,0}$ to the unknown frequencies σ_1, σ_2, respectively.

Assuming that the convergence-control parameter c_0 is properly chosen so that the Maclaurin series of $\Phi(\xi_1, \xi_2, z; q)$, $\zeta(\xi_1, \xi_2; q)$, $\Lambda_1(q)$ and $\Lambda_2(q)$ with respect to the embedding parameter q, i.e.

$$\Phi(\xi_1, \xi_2, z; q) = \sum_{m=0}^{+\infty} \varphi_m(\xi_1, \xi_2, z) q^m, \quad \zeta(\xi_1, \xi_2; q) = \sum_{m=0}^{+\infty} \eta_m(\xi_1, \xi_2) q^m, \tag{2.26a,b}$$

$$\Lambda_1(q) = \sum_{m=0}^{+\infty} \sigma_{1,m} q^m, \quad \Lambda_2(q) = \sum_{m=0}^{+\infty} \sigma_{2,m} q^m \tag{2.26c,d}$$

exist and converge at $q=1$, we have the so-called homotopy-series solution

$$\varphi(\xi_1, \xi_2, z) = \sum_{m=0}^{+\infty} \varphi_m(\xi_1, \xi_2, z), \quad \eta(\xi_1, \xi_2) = \sum_{m=0}^{+\infty} \eta_m(\xi_1, \xi_2), \tag{2.27a,b}$$

$$\sigma_1 = \sum_{m=0}^{+\infty} \sigma_{1,m}, \quad \sigma_2 = \sum_{m=0}^{+\infty} \sigma_{2,m}, \tag{2.27c,d}$$

respectively.

Substituting the Maclaurin series (2.26) into the zeroth-order deformation equations (2.20)–(2.23) and then equating the like powers of q, we obtain the so-called high-order deformation equations

$$\sum_{i=1}^{2}\sum_{j=1}^{2} \sigma_i \sigma_j \frac{\partial^2 \varphi_m}{\partial \xi_i \xi_j} - c^2 \sum_{i=1}^{2}\sum_{j=1}^{2} \boldsymbol{k}_i \cdot \boldsymbol{k}_j \frac{\partial^2 \varphi_m}{\partial \xi_i \xi_j} - c^2 \frac{\partial^2 \varphi_m}{\partial z^2} + g \frac{\partial \varphi_m}{\partial z} = 0, \quad -h \leqslant z \leqslant 0, \tag{2.28}$$

subject to the linear boundary condition

$$\mathcal{L}^*[\varphi_m] = c_0 \Delta^{\varphi}_{m-1} + \chi_m S_{m-1} - \bar{S}_m, \quad \text{on } z=0, \tag{2.29}$$

and the bottom condition

$$\frac{\partial \varphi_m}{\partial z} = 0, \quad \text{as } z \to -h, \tag{2.30}$$

together with

$$\eta_m = c_0 \Delta^{\eta}_{m-1} + \chi_m \eta_{m-1}, \quad \text{on } z = 0, \tag{2.31}$$

where $\chi_1 = 0$ and $\chi_m = 1$ for $m > 1$. $\bar{S}_m$ and S_m are dependent upon the chosen auxiliary linear operator and thus will be given later. The definitions of Δ^{φ}_{m-1} and Δ^{η}_{m-1} are given in the Appendix. Note that all of the Δ^{φ}_{m-1}, Δ^{η}_{m-1}, $\bar{S}_m$ and S_m on the right-hand side of (2.29) and (2.31) are determined by the known previous approximations η_j and φ_j $(j = 0, 1, 2, \ldots, m-1)$, and thus can be regarded as known terms.

2.3. *Small denominators of the acoustic–gravity waves*

Let $\mathcal{L}$ denote a differential operator corresponding to the linear parts of (2.12), i.e.

$$\mathcal{L}[\varphi] = \omega_1^2 \frac{\partial^2 \varphi}{\partial \xi_1^2} + 2\omega_1\omega_2 \frac{\partial^2 \varphi}{\partial \xi_1 \partial \xi_2} + \omega_2^2 \frac{\partial^2 \varphi}{\partial \xi_2^2} + g \frac{\partial \varphi}{\partial z}, \tag{2.32}$$

which has the property

$$\mathcal{L}[\Psi_{m_1,m_2}(\xi_1, \xi_2), z] = \tilde{\lambda}_{m_1,m_2} \Psi_{m_1,m_2}(\xi_1, \xi_2), \tag{2.33}$$

where

$$\tilde{\lambda}_{m_1,m_2} = \frac{g(\lambda^2_{m_1,m_2} - \gamma^2)}{\lambda_{m_1,m_2} \coth(\lambda_{m_1,m_2} h) - \gamma} - (m_1\omega_1 + m_2\omega_2)^2. \tag{2.34}$$

Therefore, its inverse operator $\mathcal{L}^{-1}$ is given by

$$\mathcal{L}^{-1}[\Psi_{m_1,m_2}(\xi_1, \xi_2, z)] = \frac{\Psi_{m_1,m_2}(\xi_1, \xi_2, z)}{\tilde{\lambda}_{m_1,m_2}}. \tag{2.35}$$

Considering the gravity wave components ($m_1 \neq m_2$), $\tilde{\lambda}_{m_1,m_2} \approx g|m_1\boldsymbol{k}_1 + m_2\boldsymbol{k}_2| - (m_1\omega_1 + m_2\omega_2)^2$. And based on (1.1), we have $k_1 \approx k_2 = k$ and $\omega_1 \approx \omega_2 = \sqrt{gk}$. For gravity wave components, when $\tilde{\lambda}_{m_1,m_2} \approx 0$, we have

$$|m_1 - m_2| - (m_1 + m_2)^2 \approx 0. \tag{2.36}$$

The above equation has an infinite number of integer solutions, as shown in table 1, corresponding to an infinite number of small denominators. Thus, it is very difficult to obtain the steady-state acoustic–gravity waves by traditional methods such as perturbation methods. Considering the hydroacoustic wave components ($m_1 = m_2$), when the resonance condition (1.3) is satisfied, one more zero denominator $\tilde{\lambda}_{1,1} = 0$ must be considered.

(m_1, m_2)	(m_1, m_2)
(1, 0)	(6, −3)
(0, 1)	(6, −10)
(1, −3)	(10, −6)
(3, −1)	(10, −15)
(3, −6)	—

TABLE 1. The values of (m_1, m_2) corresponding to $\tilde{\lambda}_{m_1,m_2} \approx 0$.

2.4. *Choice of auxiliary linear operator*

There exists an infinite number of small denominators even in the case of non-resonance. In the framework of perturbation techniques, it is rather difficult to handle such an infinite number of small denominators. However, different from perturbation methods, HAM provides us great freedom to choose the auxiliary linear operator, so that we can choose an auxiliary linear operator that is different from (2.32). Such kind of freedom of the HAM allows us to choose an appropriate auxiliary linear operator to avoid an infinite number of small denominators conveniently, as mentioned below.

Using the freedom of the HAM mentioned above, we choose such an auxiliary linear operator

$$\mathcal{L}^*[\varphi] = \omega_1^2 \frac{\partial^2 \varphi}{\partial \xi_1^2} + 2\omega_1\omega_2 \frac{\partial^2 \varphi}{\partial \xi_1 \partial \xi_2} + \omega_2^2 \frac{\partial^2 \varphi}{\partial \xi_2^2} + \mu g \frac{\partial \varphi}{\partial z}, \tag{2.37}$$

where

$$\mu = \begin{cases} 1, & m_1 = 1, m_2 = 0;\ m_1 = 0, m_2 = 1, \\ \pi/3, & \text{else}, \end{cases} \tag{2.38}$$

which has the property

$$\mathcal{L}^*[\Psi_{m_1,m_2}(\xi_1, \xi_2), z] = \tilde{\lambda}^*_{m_1,m_2} \Psi_{m_1,m_2}(\xi_1, \xi_2), \tag{2.39}$$

where

$$\tilde{\lambda}^*_{m_1,m_2} = \frac{\mu g(\lambda^2_{m_1,m_2} - \gamma^2)}{\lambda_{m_1,m_2} \coth(\lambda_{m_1,m_2} h) - \gamma} - (m_1\omega_1 + m_2\omega_2)^2. \tag{2.40}$$

So its inverse operator $\mathcal{L}^{*-1}$ reads

$$\mathcal{L}^{*-1}[\Psi_{m_1,m_2}(\xi_1, \xi_2, z)] = \frac{\Psi_{m_1,m_2}(\xi_1, \xi_2, z)}{\tilde{\lambda}^*_{m_1,m_2}}. \tag{2.41}$$

When considering the gravity wave components $(m_1 \neq m_2)$ and $\tilde{\lambda}^*_{m_1,m_2} \approx 0$, we have

$$\mu|m_1 - m_2| - (m_1 + m_2)^2 \approx 0, \tag{2.42}$$

which does not have an infinite number of integer solutions. When $m_1 = 1, m_2 = 0$ and $m_1 = 0, m_2 = 1$, the auxiliary linear operators $\mathcal{L}^*$ and $\mathcal{L}$ in (2.32) are the same, $\tilde{\lambda}^*_{1,0} = \tilde{\lambda}^*_{0,1} = 0$. For the rest, we choose $\mu = \pi/3$ as an irrational number. When $m_1 =$

m_2, $\mu|m_1-m_2|=0$, $-(m_1+m_2)^2\neq 0$. When $m_1\neq m_2$, $\mu|m_1-m_2|$ is a non-zero irrational number but $-(m_1+m_2)^2$ is a rational number, therefore it holds that $\mu|m_1-m_2|-(m_1+m_2)^2\neq 0$, because the sum of a rational number and a non-zero irrational number is always a non-zero irrational number. In this way, equation (2.42) has only two integer solutions: $m_1=1, m_2=0$ and $m_1=0, m_2=1$. Thus, we have $\tilde{\lambda}^*_{m_1,m_2}=0$ for only two cases even for resonance conditions:

$$\tilde{\lambda}^*_{1,0}=\tilde{\lambda}^*_{0,1}=0. \tag{2.43}$$

Until now, with the proper auxiliary linear operator, an infinite number of small denominators are avoided once and for all automatically. It should be emphasized that we choose two different values of μ ($\pi/3$ and $\sqrt{2}$) but obtain the same result. So, without loss of generality, we choose $\mu=\pi/3$ in the calculations of this paper.

Based on the auxiliary linear operator (2.37), $\bar{S}_m$ and S_m in high-order deformation equations are defined by

$$\bar{S}_m=\sum_{n=1}^{m-1}(\omega_1^2\beta_{2,0}^{m-n,n}+2\omega_1\omega_2\beta_{1,1}^{m-n,n}+\omega_2^2\beta_{0,2}^{m-n,n}+\mu g\gamma_{0,0}^{m-n,n}), \tag{2.44}$$

$$S_m=\omega_1^2\beta_{2,0}^{m,0}+2\omega_1\omega_2\beta_{1,1}^{m,0}+\omega_2^2\beta_{0,2}^{m,0}+\mu g\gamma_{0,0}^{m,0}+\bar{S}_m, \tag{2.45}$$

where $\beta_{i,j}^{n,m}$ and $\gamma_{i,j}^{n,m}$ are defined by (A 19) and (A 20).

2.5. *Choice of the initial guess*

In case of non-resonance, using the freedom of the HAM in the choice of the initial guess solution φ_0, we let the initial guess φ_0 contain two non-trivial components

$$\varphi_0=A\frac{g}{\omega}\Psi_{1,0}+B\frac{g}{\omega}\Psi_{0,1}, \tag{2.46}$$

where $\omega_1=\omega_2=\omega$, A and B are constants, which will be chosen for different cases. The real frequencies $\sigma_{1,0}$ and $\sigma_{2,0}$ are unknown.

In the case of resonating triads, $\tilde{\lambda}_{1,1}=0$ corresponding to the resonant hydroacoustic wave component must be considered. Assuming that the resonant hydroacoustic wave occupies a significant energy (compared to the non-resonance case) in the wave system, our strategy is to add the resonant hydroacoustic wave component to the initial guess so that the initial guess is closer to the exact solution, which will make for rapid convergence. With the great freedom in the choice of the initial guess, we let the initial guess φ_0 contain two non-trivial components and one resonant component

$$\varphi_0=A\frac{g}{\omega}\Psi_{1,0}+B\frac{g}{\omega}\Psi_{0,1}+C\frac{g}{2\omega}\Psi_{1,1}, \tag{2.47}$$

where A and B are constants, which will be chosen for different cases. C is related to A and B. It is found that, when $C=\min\{A, B\}$, convergence can be obtained in all cases in which the steady-state resonant acoustic–gravity waves exist in the present paper.

3. Results analysis

3.1. *Non-resonant waves*

For acoustic–gravity waves far from resonance, we take the same case as that considered by Kadri & Stiassnie (2013):

$$\boldsymbol{k}_1 = (0.101937, 0)\ \mathrm{m}^{-1}, \quad \omega_1 = 1.0\ \mathrm{s}^{-1}, \tag{3.1a}$$

$$\boldsymbol{k}_2 = (-0.101937, 0)\ \mathrm{m}^{-1}, \quad \omega_2 = 1.0\ \mathrm{s}^{-1}, \tag{3.1b}$$

$$\boldsymbol{k}_3 = (0, 0)\ \mathrm{m}^{-1}, \quad \omega_3 = 2.0\ \mathrm{s}^{-1}, \tag{3.1c}$$

where the water depth h is equal to 4000 m. Based on the perturbed equation of the second-order interaction, Kadri & Stiassnie (2013) investigated the two primary gravity waves and the resulting hydroacoustic wave in the whole system (without considering an infinite number of zero denominators). For this case, from equation (8.2) of Kadri & Stiassnie (2013) after adding more significant digits, it gives

$$|A^{(3)}| = 0.20481|A^{(1)}||A^{(2)}|, \tag{3.2}$$

where $A^{(i)}$ represents the wave amplitude. For the same case, we get a convergent solution by choosing $A = B = 1/10$ m in the initial guess

$$|A^{(3)}| = 0.20482|A^{(1)}||A^{(2)}|. \tag{3.3}$$

There is a slight difference between (3.2) and (3.3), because Kadri & Stiassnie (2013) considered the second-order equations of the boundary condition on the free surface but we consider the fully nonlinear boundary condition. This illustrates the validity of our HAM approach.

3.2. *Resonant waves*

The resonant triad interactions of acoustic–gravity waves exist at special water depths $h \approx (n + 0.5)\pi c/\omega_3$, as mentioned by Longuet-Higgins (1950). From $h \approx (n + 0.5)\pi c/\omega_3$, we have

$$\omega_3 \approx (n + 0.5)\pi c/h. \tag{3.4}$$

Substituting $c = 1500\ \mathrm{m\ s^{-1}}$ and $h = 4000$ m into the above algebraic equation, we have

$$\omega_3 \approx 1.17810(n + 0.5). \tag{3.5}$$

When $n = 0, 1, 2, 3, \ldots$, $\omega_3 \approx 0.589049\ \mathrm{s}^{-1}, 1.76715\ \mathrm{s}^{-1}, 2.94529\ \mathrm{s}^{-1}, 4.12334\ \mathrm{s}^{-1}, \ldots$, respectively. Actually, we can get the convergent solution of the steady-state acoustic–gravity waves for the cases of mode $n = 1$ and mode $n = 2$, but not for the cases of mode $n = 0$ and mode $n = 3$. This illustrates that steady-state resonant acoustic–gravity waves do not exist in all cases, as Xu *et al.* (2012) mentioned for general steady-state resonant gravity waves. We obtain the cases of exact resonating triads in a way similar to that of Kadri & Stiassnie (2013).

i	$\sigma_{1,0}$ (s^{-1})	$\sigma_{2,0}$ (s^{-1})
Group 1	−0.883375	−0.880457
Group 2	−0.883375	0.887434
Group 3	0.884491	−0.880457
Group 4	0.884491	0.887434

TABLE 2. The solution of (3.8) in the case of $h=4000$ m, $k_1=k_2=0.0796449\ \text{m}^{-1}$, $A=1/20$ m, $B=1/50$ m, $C=1/50$ m.

3.2.1. *Resonant waves for the case with* $|\boldsymbol{k}_3|=0$ *(mode* $n=1$*)*

For the resonant waves, we consider first the case of Longuet-Higgins with $|\boldsymbol{k}_3|=0$ and present detailed results for mode $n=1$ near the non-resonance case we considered in § 3.1, say, $\omega_3 = 1.76784\ \text{s}^{-1}$. So, we investigate here the following resonant acoustic–gravity wave system:

$$\boldsymbol{k}_1=(0.0796449, 0)\ \text{m}^{-1},\quad \omega_1=0.883921\ \text{s}^{-1}, \tag{3.6a}$$

$$\boldsymbol{k}_2=(-0.0796449, 0)\ \text{m}^{-1},\quad \omega_2=0.883921\ \text{s}^{-1}, \tag{3.6b}$$

$$\boldsymbol{k}_3=(0, 0)\ \text{m}^{-1},\quad \omega_3=1.76784\ \text{s}^{-1}. \tag{3.6c}$$

In this case, we choose $A=1/20$ m, $B=1/50$ m and $C=\min\{A, B\}=1/50$ m in the initial guess (2.47).

Substituting this initial guess into the so-called first-order deformation equation (2.29) ($m=1$) in the framework of HAM, we have

$$\begin{aligned}\mathcal{L}^*[\varphi_1] &= c_0\Delta_0^{\varphi}-\bar{S}_1\\ &= \bar{b}_{1,0}\sin(\xi_1)+\bar{b}_{0,1}\sin(\xi_2)+\bar{b}_{2,0}\sin(2\xi_1)+\bar{b}_{0,2}\sin(2\xi_2)\\ &\quad+\bar{b}_{1,1}\sin(\xi_1+\xi_2)+\bar{b}_{1,-1}\sin(\xi_1-\xi_2)+\bar{b}_{2,1}\sin(2\xi_1+\xi_2)+\bar{b}_{1,2}\sin(\xi_1+2\xi_2)\\ &\quad+\bar{b}_{3,1}\sin(3\xi_1+\xi_2)+\bar{b}_{2,2}\sin(2\xi_1+2\xi_2)+\bar{b}_{1,3}\sin(\xi_1+3\xi_2)\\ &\quad+\bar{b}_{3,2}\sin(3\xi_1+2\xi_2)+\bar{b}_{2,3}\sin(2\xi_1+3\xi_2)+\bar{b}_{3,3}\sin(3\xi_1+3\xi_2),\end{aligned} \tag{3.7}$$

where $\bar{b}_{m_1,m_2}$ depends upon $\sigma_{1,0}$, $\sigma_{2,0}$, which is unknown in the initial guess (2.47). Owing to the property of the inverse linear operator (2.41), the coefficients of the terms $\sin(\xi_1)$ and $\sin(\xi_2)$ on the right-hand side of the first-order deformation equation (2.29) ($m=1$) must be zero so as to avoid secular terms. This provides two coupled nonlinear algebraic equations for $\sigma_{1,0}$, $\sigma_{2,0}$

$$0.433575+0.000619520\sigma_{1,0}-0.554914\sigma_{1,0}^2=0, \tag{3.8a}$$

$$0.173432+0.000154880\sigma_{2,0}-0.221965\sigma_{2,0}^2=0, \tag{3.8b}$$

whose solutions are shown in table 2. Since $\sigma_{1,0}$, $\sigma_{2,0}$ must be positive, only group 4 has physical meaning. As long as $\sigma_{1,0}$, $\sigma_{2,0}$ are determined, φ_0 is known. And, with the initial guess $\eta_0=0$, it is straightforward to calculate η_1 directly. We have

$$\begin{aligned}\eta_1 &= c_0\Delta_0^{\eta}\\ &= \bar{a}_{1,0}\cos(\xi_1)+\bar{a}_{0,1}\cos(\xi_2)+\bar{a}_{1,1}\cos(\xi_1+\xi_2)\\ &\quad+\bar{a}_{2,1}\cos(2\xi_1+\xi_2)+\bar{a}_{1,2}\cos(\xi_1+2\xi_2),\end{aligned} \tag{3.9}$$

where $\bar{a}_{m_1,m_2}$ are known constants.

Now, all terms on the right-hand side of the first-order deformation equation (2.29) ($m=1$) are known, so it is straightforward to obtain φ_1:

$$\varphi_1 = \mathcal{L}^{*-1}[c_0 \Delta_0^{\varphi} - \bar{S}_1] + A^* \Psi_{1,0} + B^* \Psi_{0,1}. \tag{3.10}$$

Since the components $A(\omega/g)\Psi_{1,0}$ and $B(\omega/g)\Psi_{0,1}$ of the two primary waves are given, we have $A^* = B^* = 0$ so that

$$\begin{aligned} \varphi_1 &= \mathcal{L}^{*-1}[c_0 \Delta_0^{\varphi} - \bar{S}_1] \\ &= \bar{d}_{1,0}\Psi_{1,0} + \bar{d}_{0,1}\Psi_{0,1} + \bar{d}_{2,0}\Psi_{2,0} + \bar{d}_{0,2}\Psi_{0,2} + \bar{d}_{1,1}\Psi_{1,1} + \bar{d}_{1,-1}\Psi_{1,-1} + \bar{d}_{2,1}\Psi_{2,1} \\ &\quad + \bar{d}_{1,2}\Psi_{1,2} + \bar{d}_{3,1}\Psi_{3,1} + \bar{d}_{2,2}\Psi_{2,2} + \bar{d}_{1,3}\Psi_{1,3} + \bar{d}_{3,2}\Psi_{3,2} + \bar{d}_{2,3}\Psi_{2,3} + \bar{d}_{3,3}\Psi_{3,3}, \end{aligned} \tag{3.11}$$

where $\bar{d}_{m_1,m_2} = \bar{b}_{m_1,m_2}/\tilde{\lambda}^*_{m_1,m_2}$. We substitute φ_1 into the second-order deformation equation (2.29) ($m=2$). Note that coefficients of $\sin(m_1\xi_1 + m_2\xi_2)$ contain $\sigma_{1,1}$ and $\sigma_{2,1}$ that are unknown right now. Then, enforcing the coefficients of $\sin(\xi_1)$ and $\sin(\xi_2)$ on its right-hand side to be zero so as to avoid secular terms, we can further determine $\sigma_{1,1}$ and $\sigma_{2,1}$ in a similar way. Then, we can similarly obtain η_2, φ_2, and so on.

In addition, the 'convergence-control parameter' c_0 can provide a convenient way to guarantee the convergence of the solution series in the framework of HAM. The optimal value of c_0 is determined through the minimum residuals of (2.12) and (2.13) to guarantee the convergence of the HAM approximations. Define the averaged residual square as

$$\varepsilon_m^{\phi} = \frac{1}{\pi^2}\int_0^{\pi}\int_0^{\pi}\left(\sum_{n=0}^{m}\Delta_n^{\phi}\right)^2 \mathrm{d}\xi_1\,\mathrm{d}\xi_2, \tag{3.12}$$

$$\varepsilon_m^{\eta} = \frac{1}{\pi^2}\int_0^{\pi}\int_0^{\pi}\left(\sum_{n=0}^{m}\Delta_n^{\eta}\right)^2 \mathrm{d}\xi_1\,\mathrm{d}\xi_2, \tag{3.13}$$

for the mth-order approximation of ϕ and η. The residual errors of ε_m^{ϕ} and ε_m^{η} both decrease sharply when the value of c_0 is close to -1.35, as shown in figure 1. Then, we choose $c_0 = -1.35$. The corresponding residual error squares of the two boundary conditions decease rather quickly to the level 10^{-16} at 20th order, as shown in table 3 and figure 2. Then, we can obtain the convergent wave frequencies and amplitudes, which are given in table 4. The $a^*_{1,1}$ represents the amplitude corresponding to the resonant hydroacoustic wave component. If we neglect the $g(\partial\varphi/\partial z)$ term in (2.1), we can also get the convergent series solutions of the steady-state resonant acoustic–gravity waves, as shown in table 5. It is found that the gravity contribution in (2.1) is very small. The existence of $g(\partial\varphi/\partial z)$ has negligible effect on the calculation results of this paper. Actually, one can omit the gravity contribution in (2.1) for practical purposes. This conclusion was also confirmed by Abdolali & Kirby (2017), who showed the negligible role of $g(\partial\varphi/\partial z)$ on hydroacoustic waves and surface gravity waves with short wavelength. Furthermore, we investigate different cases in a similar way, as shown in table 6.

Define

$$\Pi = \sum_{m_1=0}^{+\infty}\sum_{m_2=-\infty}^{+\infty}(a_{m_1,m_2})^2. \tag{3.14}$$

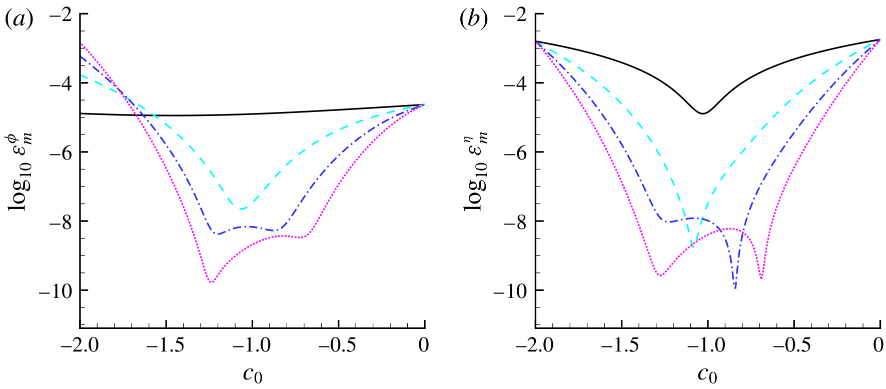

FIGURE 1. (Colour online) Averaged residual squares versus c_0 in the case of $h = 4000$ m, $k_1 = k_2 = 0.0796449$ m^{-1}, $A = 1/20$ m, $B = 1/50$ m, $C = 1/50$ m. Solid line: first-order approximation; dashed line: third-order approximation; dash-dot-dotted line: fifth-order approximation; dotted line: seventh-order approximation. Panel (*a*) represents averaged residual square of $\log_{10}\varepsilon_m^{\phi}$ versus c_0 and (*b*) represents averaged residual square of $\log_{10}\varepsilon_m^{\eta}$ versus c_0.

m (order of approximation)	ε_m^{ϕ}	ε_m^{η}
1	0.00002130	0.00164865
5	5.70×10^{-7}	4.86×10^{-7}
10	5.84×10^{-10}	1.13×10^{-10}
15	7.94×10^{-13}	1.13×10^{-13}
20	9.76×10^{-16}	1.47×10^{-16}

TABLE 3. The averaged residual squares of ε_m^{ϕ} and ε_m^{η} in the case of $h = 4000$ m, $k_1 = k_2 = 0.0796449$ m^{-1}, $A = 1/20$ m, $B = 1/50$ m, $C = 1/50$ m by means of $c_0 = -1.35$.

m	ϵ_1	ϵ_2	$a_{1,0}$	$a_{0,1}$	$a^*_{1,1}$
1	1.000645	1.003974	0.0675009	0.0270007	0.0267706
5	0.999196	0.994859	0.0502925	0.0201725	0.0263204
10	0.999170	0.994775	0.0500194	0.0200514	0.0261579
15	0.999171	0.994776	0.0500211	0.0200522	0.0261548
18	0.999171	0.994776	0.0500210	0.0200522	0.0261547
20	0.999171	0.994777	0.0500210	0.0200522	0.0261546
21	0.999171	0.994777	0.0500210	0.0200522	0.0261546

TABLE 4. Analytical approximations of the dimensional angular frequencies and wave amplitude components (m) in the case of $k_1 = k_2 = 0.0796449$ m^{-1}, $A = 1/20$ m, $B = 1/50$ m, $C = 1/50$ m.

The wave amplitudes and energy distributions of the two primary waves and resonant hydroacoustic wave component are given in table 7. It is found that the two primary gravity waves and the resonant hydroacoustic wave as a whole occupy most wave energy in all considered cases. A similar conclusion was found for steady-state

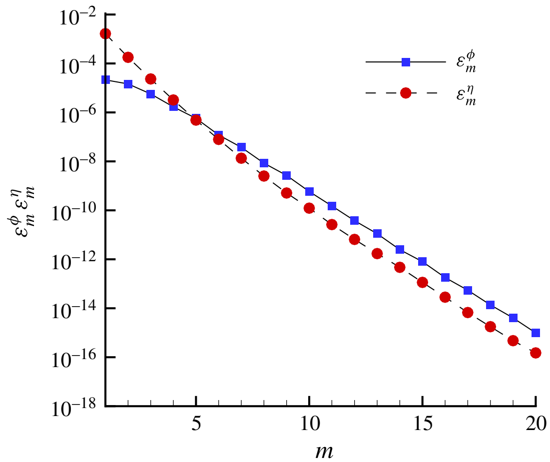

FIGURE 2. (Colour online) Averaged residual squares of ε_m^ϕ and ε_m^η versus the approximation order m by means of $c_0 = -1.35$ in the case of $h = 4000$ m, $k_1 = k_2 = 0.0796449$ m^{-1}, $A = 1/20$ m, $B = 1/50$ m, $C = 1/50$ m.

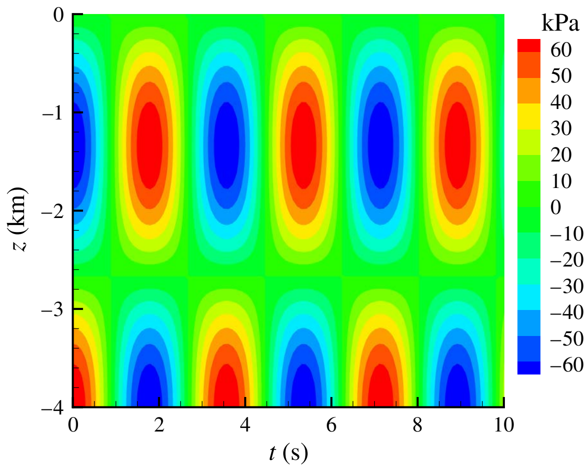

FIGURE 3. (Colour online) Time variation of dynamic pressure (p_d) induced by the resulting hydroacoustic wave in the case $k_1 = k_2 = 0.0796449$ m^{-1}, $A = 1/20$ m, $B = 1/50$ m, $C = 1/50$ m.

exactly/nearly resonant gravity waves by Liao (2011*b*), Xu *et al.* (2012), Liu & Liao (2014), Liu *et al.* (2015) and Liao *et al.* (2016).

Next, we discuss the pressure distribution of the steady-state resonant acoustic–gravity waves. We consider here the dynamic pressure p_d of the resulting hydroacoustic wave in the whole fluid. Figure 3 shows the time variation of dynamic pressure (p_d) induced by the hydroacoustic wave in the case $k_1 = k_2 = 0.0796449$ m^{-1}, $A = 1/20$ m, $B = 1/50$ m. It is found that, when the resonance condition is exactly satisfied, acoustic–gravity waves can also generate a periodic pressure on the ocean floor, whose frequency is the superposition of the actual wave frequencies of the two primary waves. If the amplitudes of the two primary waves are the same (the cases

	ϵ_1	ϵ_2	$a_{1,0}$	$a_{0,1}$	$a^*_{1,1}$
With $g\dfrac{\partial\varphi}{\partial z}$	0.999171	0.994777	0.0500210	0.0200522	0.0261546
Without $g\dfrac{\partial\varphi}{\partial z}$	0.999171	0.994773	0.0500211	0.0200522	0.0261541

TABLE 5. The dimensionless angular frequencies and the wave amplitude components (m) in the case with $|\boldsymbol{k}_3| = 0$ (mode $n = 1$), $A = 1/20$ m and $B = 1/50$ m with or without the $g(\partial\varphi/\partial z)$ term in (2.1).

A	B	ϵ_1	ϵ_2	$a_{1,0}$	$a_{0,1}$	$a^*_{1,1}$
1/10	1/10	0.992044	0.992044	0.1004001	0.1004001	0.0993025
1/20	1/20	0.996020	0.996020	0.0500998	0.0500998	0.0498267
1/20	1/25	0.997190	0.995603	0.0500706	0.0400881	0.0440260
1/20	1/50	0.999171	0.994777	0.0500210	0.0200522	0.0261546
1/20	1/100	0.999787	0.994487	0.0500056	0.0100275	0.0138027

TABLE 6. The dimensionless angular frequencies and the wave amplitude components (m) versus A (m) and B (m) in the case of $k_1 = k_2 = 0.0796449$ m^{-1}.

A	B	$a^2_{1,0}/\Pi$ (%)	$a^2_{0,1}/\Pi$ (%)	$a^{*2}_{1,1}/\Pi$ (%)
1/10	1/10	33.57	33.57	32.84
1/20	1/20	33.45	33.45	33.09
1/20	1/25	41.42	26.55	32.02
1/20	1/50	69.73	11.21	19.06
1/20	1/100	89.57	3.60	6.82

TABLE 7. The energy distribution of the wave system versus A (m) and B (m) in the case of $k_1 = k_2 = 0.0796449$ m^{-1}.

corresponding to $A = B$ in the initial guess φ_0), the actual wave frequencies of the two primary waves are the same. So, the frequency of the pressure at the sea bottom is exactly twice the wave frequency of the primary gravity waves. The pressure generated by the acoustic–gravity waves is dependent of the water depth, as shown in figure 3. The magnitude of pressure is related to the amplitude of the hydroacoustic wave, which is determined by the value of A and B in the initial guess of the velocity potential φ_0. In the present case, the maximum dynamic pressure on the bottom is approximately 70 kPa, which is much larger than the pressure ($\approx$3.5 Pa) obtained in the above-mentioned case of non-resonance with the same amplitude $A = 1/20$ m and $B = 1/50$ m of the velocity potential φ_0. This value is of the same order of magnitude as the maximum dynamic pressure of the first acoustic–gravity wave mode generated by bottom motion in the study of Oliveira & Kadri (2016). So, the resonant acoustic–gravity waves might indeed trigger microseisms in the Earth.

Without considering the compressibility of the water, Pellet *et al.* (2017) obtained a second-order pressure field generated by two exactly opposite travelling gravity waves ($\boldsymbol{k}_1 + \boldsymbol{k}_2 = \boldsymbol{0}$), which is independent of water depth and periodic in time with twice the frequency of the primary gravity waves. It reads

$$p_2 = 8\rho\omega_1^2 a_{1,0} a_{0,1} \cos(2\omega_1 t). \tag{3.15}$$

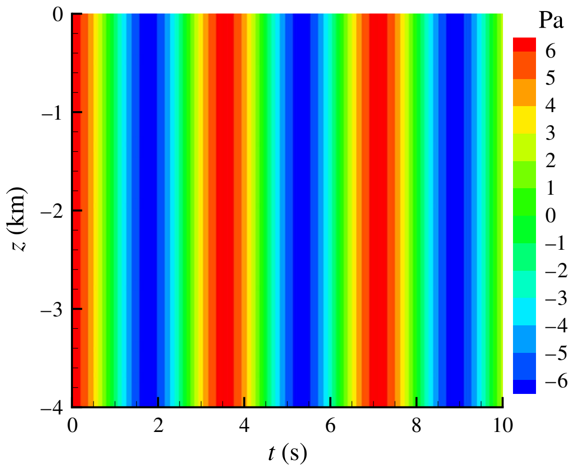

FIGURE 4. (Colour online) The second-order pressure induced by two opposite primary waves in the case of $\omega_1 = 0.884266\ \mathrm{s}^{-1}$, $a_{1,0} = 0.0500210$ m, $a_{0,1} = 0.0200522$ m.

We choose the same amplitudes of the two primary waves as these in the resonance case (3.6). $a_{1,0} = 0.0500210$ m, $a_{0,1} = 0.0200522$ m. Then we can get the second-order pressure field, as shown in figure 4. The second-order pressure is proportional to the amplitudes of the two primary waves. It is found that when the acoustic–gravity waves resonance occurs, the maximum dynamic pressure on the bottom is approximately 70 kPa (with compressibility), which is much larger than the second-order pressure (≈6 Pa) (without compressibility) obtained with the same amplitudes of the two primary waves. The reason is that no resonance occurs in the whole system, when we ignore the compressibility of water.

3.2.2. *Resonant waves for the case with* $|\boldsymbol{k}_3| = 0$ *(mode* $n = 2$*)*

Here, we investigate the following resonant acoustic–gravity wave system (mode $n = 2$):

$$\boldsymbol{k}_1 = (0.221124, 0)\ \mathrm{m}^{-1}, \quad \omega_1 = 1.47283\ \mathrm{s}^{-1}, \tag{3.16a}$$

$$\boldsymbol{k}_2 = (-0.221124, 0)\ \mathrm{m}^{-1}, \quad \omega_2 = 1.47283\ \mathrm{s}^{-1}, \tag{3.16b}$$

$$\boldsymbol{k}_3 = (0, 0)\ \mathrm{m}^{-1}, \quad \omega_3 = 2.94566\ \mathrm{s}^{-1}. \tag{3.16c}$$

In this case, we choose $A = 1/50$ m and different values of B in the initial guess (2.47). The dimensionless angular frequencies and the wave amplitude components in different conditions are shown in table 8. Similarly to the results of case (3.6), it is found that the two primary gravity waves and the resonant hydroacoustic wave as a whole occupy most wave energy in all considered cases, as shown in table 9. The dynamic pressure p_d of the resulting hydroacoustic wave in the whole fluid in the case of $A = 1/50$ m and $B = 1/100$ m is shown in figure 5. The maximum dynamic pressure on the bottom is approximately 55 kPa, which might indeed trigger microseisms of the ocean floor.

3.2.3. *Resonant waves for the case with* $0 < |\boldsymbol{k}_3| < \omega_3/c$

The resonance case (mode $n = 1$) given by Kadri & Stiassnie (2013) is

$$\boldsymbol{k}_1 = (0.102249, 0)\ \mathrm{m}^{-1}, \quad \omega_1 = 1.00153\ \mathrm{s}^{-1}, \tag{3.17a}$$

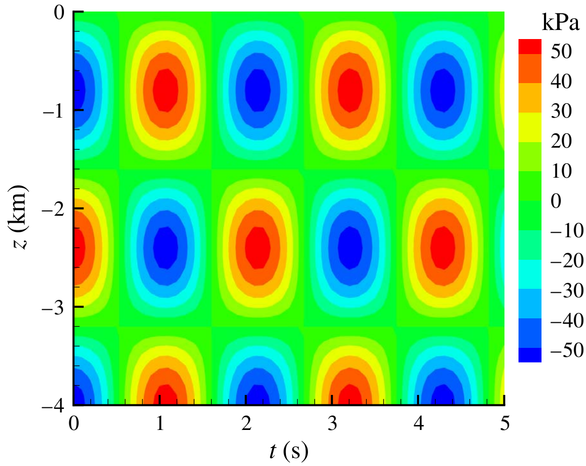

FIGURE 5. (Colour online) Time variation of dynamic pressure (p_d) induced by the resulting hydroacoustic wave in the case $k_1 = k_2 = 0.221124\ \mathrm{m}^{-1}$, $A = 1/50$ m, $B = 1/100$ m.

B	ϵ_1	ϵ_2	$a_{1,0}$	$a_{0,1}$	$a^*_{1,1}$
1/50	0.995880	0.995880	0.0200443	0.0200443	0.0199223
1/100	0.998610	0.994410	0.0200141	0.0100279	0.0125962
1/150	0.999350	0.994075	0.0200067	0.0066864	0.0089018

TABLE 8. The dimensionless angular frequencies and the wave amplitude components (m) versus B (m) in the case of $k_1 = k_2 = 0.221124\ \mathrm{m}^{-1}$, $A = 1/50$ m.

B	$a^2_{1,0}/\Pi$ (%)	$a^2_{0,1}/\Pi$ (%)	$a^{*2}_{1,1}/\Pi$ (%)
1/50	33.47	33.47	33.06
1/100	60.71	15.24	24.05
1/150	76.35	8.53	15.12

TABLE 9. The energy distribution of the wave system versus B (m) in the case of $k_1 = k_2 = 0.221124\ \mathrm{m}^{-1}$, $A = 1/50$ m.

$$\boldsymbol{k}_2 = (-0.101625, 0)\ \mathrm{m}^{-1}, \quad \omega_2 = 0.99847\ \mathrm{s}^{-1}, \tag{3.17b}$$
$$\boldsymbol{k}_3 = (0.000642, 0)\ \mathrm{m}^{-1}, \quad \omega_3 = 2.00000\ \mathrm{s}^{-1}. \tag{3.17c}$$

For studying this resonance case, we choose $A = 1/20$ m and different values of B in the initial guess (2.47). We can obtain the convergent wave frequencies and amplitudes through the same calculation process as in § 3.2.1, as shown in table 10. The energy distributions of the wave system are shown in table 11. It is found that the convergent solutions of the resonance steady-state acoustic–gravity triads for general resonance case with $0 < |\boldsymbol{k}_3| < \omega_3/c$ can even be obtained. This illustrates the generality of the existence of the steady-state resonant acoustic–gravity waves. And the two primary gravity waves along with the resonant hydroacoustic wave as a whole occupy most wave energy in the wave system like (3.6) and (3.16) with $|\boldsymbol{k}_3| = 0$.

B	ϵ_1	ϵ_2	$a_{1,0}$	$a_{0,1}$	$a^*_{1,1}$
1/20	0.994907	0.994906	0.0501282	0.0501274	0.0497762
1/25	0.996404	0.994372	0.0500907	0.0401124	0.0439924
1/50	0.998941	0.993313	0.0500271	0.0200666	0.0261387
1/100	0.999730	0.992943	0.0500073	0.0100351	0.0137940

TABLE 10. The dimensionless angular frequencies and the wave amplitude components (m) versus B (m) in the case of $k_1 = 0.102249\ \mathrm{m}^{-1}$, $k_2 = 0.101625\ \mathrm{m}^{-1}$, $A = 1/20$ m.

B	$a^2_{1,0}/\Pi$ (%)	$a^2_{0,1}/\Pi$ (%)	$a^{*2}_{1,1}/\Pi$ (%)
1/20	33.49	33.49	33.02
1/25	41.45	26.58	31.97
1/50	69.74	11.22	19.04
1/100	89.58	3.61	6.81

TABLE 11. The energy distribution of the wave system versus B (m) in the case of $k_1 = 0.102249\ \mathrm{m}^{-1}$, $k_2 = 0.101625\ \mathrm{m}^{-1}$, $A = 1/20$ m.

Even in the cases of $h = 2000$ m and $h = 3000$ m, we also obtain the steady-state resonant acoustic–gravity waves. It means that steady-state resonant acoustic–gravity waves commonly exist in water of uniform depth. This agrees with Kadri & Stiassnie (2013), who pointed out that the water depth h should be greater than $h_{cr} \equiv \pi c/2\omega_3$ for the existence of a hydroacoustic wave.

4. Concluding remarks and discussion

The steady-state acoustic–gravity waves are studied under non-resonance and exact resonance conditions. In the framework of traditional methods, like the perturbation methods, there exist an infinite number of small denominators. However, in the framework of HAM, these infinite number of small denominators can be avoided conveniently by means of choosing a piecewise auxiliary linear operator. Besides, the so-called convergence-control parameter provides a simple way to guarantee the convergence of solution series. Considering the works of Liao (2011*b*), Xu *et al.* (2012), Liu & Liao (2014), Liu *et al.* (2015), Liao *et al.* (2016) and Liu *et al.* (2018), the steady-state waves with time-independent wave spectrum commonly exist not only for gravity waves in various depths of water but also for acoustic–gravity waves in deep water of uniform depth.

In the considered case without resonance, the solutions given by our HAM approach agree well with those obtained by Kadri & Stiassnie (2013). This illustrates the validity of our HAM approach. In the considered cases with resonance, steady-state resonant acoustic–gravity waves have been obtained for the first time, to the best of our knowledge. Like the steady-state resonant gravity waves (Xu *et al.* 2012; Liu & Liao 2014; Liu *et al.* 2015; Liao *et al.* 2016), the two primary gravity waves and the resonant acoustic–gravity occupy most of wave energy. This illustrates the common existence of the steady-state resonant waves.

When dealing with the pressure field caused by the hydroacoustic waves, most of researchers considered the non-resonant acoustic–gravity waves and the hydroacoustic waves generated by the vertical oscillations of ocean floor. For the resonance state, no specific analysis of the pressure field was given. In this paper, we obtained the steady-state acoustic–gravity waves under the exact resonance criterion. So, it is easy for us to get the pressure field caused by the steady-state resonant hydroacoustic wave component. It is found that the resonant acoustic–gravity waves can indeed generate a pressure on the ocean floor, the frequency of which is the superposition of the actual wave frequencies of the two primary waves. The maximum dynamic pressure on the bottom is much larger than the pressure in the case of non-resonance and the second-order pressure without considering the compressibility of the water, which might trigger microseisms in the Earth.

In addition, we also successfully obtained the steady-state resonant acoustic–gravity waves in some cases with different water depths, such as $h = 3000$ m and $h = 2000$ m. This indicates that the steady-state resonant acoustic–gravity waves commonly exist in deep water of uniform depth. The steady-state resonant acoustic–gravity waves obtained in this paper are helpful to enrich our understanding about resonant acoustic–gravity waves.

Acknowledgements

We are grateful to the National Natural Science Foundation of China (approval no. 11432009) for financial support. This work is also partly supported by the Lloyd's Register Foundation (LRF). Lloyd's Register Foundation works on achieving advances in engineering-related education, public engagement and the application of research to protect life and property. F.D. was partially funded through the US-Ireland Research & Development Partnership Programme as part of the collaborative project 'Understanding Extreme Nearshore Wave Events through Studies of Coastal Boulder Transport' (grant nos 14/US/E3111 and NSF 1529756).

Appendix A. Definitions of Δ_m^{φ} and Δ_m^{η} in (2.29) and (2.31)

The definitions of Δ_m^{φ} and Δ_m^{η} in (2.29) and (2.31) are given by

$$\Delta_m^{\varphi} = O_m + g\bar{\varphi}_{z,m}^{0,0} - 2H_m + \Lambda_m, \tag{A 1}$$

$$\Delta_m^{\eta} = \eta_m - \frac{1}{g}\Upsilon_m, \tag{A 2}$$

where

$$O_m = \sum_{n=0}^{m}(K_{n,1}\bar{\varphi}_{m-n}^{2,0} + 2K_{n,3}\bar{\varphi}_{m-n}^{1,1} + K_{n,2}\bar{\varphi}_{m-n}^{0,2}), \tag{A 3}$$

$$H_m = \sum_{n=0}^{m}(\sigma_{1,n}\Gamma_{m-n,1} + \sigma_{2,n}\Gamma_{m-n,2}), \tag{A 4}$$

$$\begin{aligned}\Lambda_m &= \sum_{n=0}^{m}(k_1^2\bar{\varphi}_n^{1,0}\Gamma_{m-n,1} + k_2^2\bar{\varphi}_n^{0,1}\Gamma_{m-n,2} + \bar{\varphi}_{z,n}^{0,0}\Gamma_{m-n,3}) \\ &\quad + \boldsymbol{k}_1\cdot\boldsymbol{k}_2\sum_{n=0}^{m}(\bar{\varphi}_n^{1,0}\Gamma_{m-n,2} + \bar{\varphi}_n^{0,1}\Gamma_{m-n,1}),\end{aligned} \tag{A 5}$$

$$\Upsilon_m = \sum_{n=0}^{m}(\sigma_{1,n}\bar{\varphi}_{m-n}^{1,0} + \sigma_{2,n}\bar{\varphi}_{m-n}^{0,1}) - \Gamma_{m,0}, \tag{A 6}$$

with the definitions

$$K_{n,1}=\sum_{m=0}^{n}\sigma_{1,m}\sigma_{1,n-m}, \tag{A 7}$$

$$K_{n,2}=\sum_{m=0}^{n}\sigma_{2,m}\sigma_{2,n-m}, \tag{A 8}$$

$$K_{n,3}=\sum_{m=0}^{n}\sigma_{1,m}\sigma_{2,n-m}, \tag{A 9}$$

$$\begin{aligned}\Gamma_{m,0} &= \frac{k_1^2}{2}\sum_{n=0}^{m}\bar{\varphi}_n^{1,0}\bar{\varphi}_{m-n}^{1,0}+\boldsymbol{k}_1\cdot\boldsymbol{k}_2\sum_{n=0}^{m}\bar{\varphi}_n^{1,0}\bar{\varphi}_{m-n}^{0,1}+\frac{k_2^2}{2}\sum_{n=0}^{m}\bar{\varphi}_n^{0,1}\bar{\varphi}_{m-n}^{0,1}\\ &\quad +\frac{1}{2}\sum_{n=0}^{m}\bar{\varphi}_{z,n}^{0,0}\bar{\varphi}_{z,m-n}^{0,0},\end{aligned} \tag{A 10}$$

$$\begin{aligned}\Gamma_{m,1} &= \sum_{n=0}^{m}(k_1^2\bar{\varphi}_n^{1,0}\bar{\varphi}_{m-n}^{2,0}+k_2^2\bar{\varphi}_n^{0,1}\bar{\varphi}_{m-n}^{1,1}+\bar{\varphi}_{z,n}^{0,0}\bar{\varphi}_{z,m-n}^{1,0})\\ &\quad +\boldsymbol{k}_1\cdot\boldsymbol{k}_2\sum_{n=0}^{m}(\bar{\varphi}_n^{1,0}\bar{\varphi}_{m-n}^{1,1}+\bar{\varphi}_n^{2,0}\bar{\varphi}_{m-n}^{0,1}),\end{aligned} \tag{A 11}$$

$$\begin{aligned}\Gamma_{m,2} &= \sum_{n=0}^{m}(k_1^2\bar{\varphi}_n^{1,0}\bar{\varphi}_{m-n}^{1,1}+k_2^2\bar{\varphi}_n^{0,1}\bar{\varphi}_{m-n}^{0,2}+\bar{\varphi}_{z,n}^{0,0}\bar{\varphi}_{z,m-n}^{0,1})\\ &\quad +\boldsymbol{k}_1\cdot\boldsymbol{k}_2\sum_{n=0}^{m}(\bar{\varphi}_n^{1,0}\bar{\varphi}_{m-n}^{0,2}+\bar{\varphi}_n^{0,1}\bar{\varphi}_{m-n}^{1,1}),\end{aligned} \tag{A 12}$$

$$\begin{aligned}\Gamma_{m,3} &= \sum_{n=0}^{m}(k_1^2\bar{\varphi}_n^{1,0}\bar{\varphi}_{z,m-n}^{1,0}+k_2^2\bar{\varphi}_n^{0,1}\bar{\varphi}_{z,m-n}^{0,1}+\bar{\varphi}_{z,n}^{0,0}\bar{\varphi}_{zz,m-n}^{0,0})\\ &\quad +\boldsymbol{k}_1\cdot\boldsymbol{k}_2\sum_{n=0}^{m}(\bar{\varphi}_n^{1,0}\bar{\varphi}_{z,m-n}^{0,1}+\bar{\varphi}_n^{0,1}\bar{\varphi}_{z,m-n}^{1,0}).\end{aligned} \tag{A 13}$$

The expressions for $\bar{\varphi}_n^{i,j}$, $\bar{\varphi}_{z,n}^{i,j}$ and $\bar{\varphi}_{zz,n}^{i,j}$ are

$$\bar{\varphi}_n^{i,j}=\sum_{m=0}^{n}\beta_{i,j}^{n-m,m}, \tag{A 14}$$

$$\bar{\varphi}_{z,n}^{i,j}=\sum_{m=0}^{n}\gamma_{i,j}^{n-m,m}, \tag{A 15}$$

$$\bar{\varphi}_{zz,n}^{i,j}=\sum_{m=0}^{n}\delta_{i,j}^{n-m,m}, \tag{A 16}$$

with the definitions

$$\mu_{m,n}=\begin{cases}\eta_n, & m=1,\, n\geqslant 1,\\ \displaystyle\sum_{i=m-1}^{n-1}\mu_{m-1,i}\eta_{n-i}, & m\geqslant 2,\, n\geqslant m,\end{cases} \tag{A 17}$$

$$\psi_{i,j}^{n,m} = \frac{\partial^{i+j}}{\partial {\xi_1}^i \partial {\xi_2}^j} \left(\frac{1}{m!} \left. \frac{\partial \varphi_n}{\partial z^m} \right|_{z=0} \right), \tag{A 18}$$

$$\beta_{i,j}^{n,m} = \begin{cases} \psi_{i,j}^{n,0}, & m = 0, \\ \displaystyle\sum_{s=1}^{m} \psi_{i,j}^{n,s} \mu_{s,m}, & m \geqslant 1, \end{cases} \tag{A 19}$$

$$\gamma_{i,j}^{n,m} = \begin{cases} \psi_{i,j}^{n,1}, & m = 0, \\ \displaystyle\sum_{s=1}^{m} (s+1) \psi_{i,j}^{n,s+1} \mu_{s,m}, & m \geqslant 1, \end{cases} \tag{A 20}$$

$$\delta_{i,j}^{n,m} = \begin{cases} 2\psi_{i,j}^{n,2}, & m = 0, \\ \displaystyle\sum_{s=1}^{m} (s+1)(s+2) \psi_{i,j}^{n,s+2} \mu_{s,m}, & m \geqslant 1. \end{cases} \tag{A 21}$$

A detailed derivation can be found in the appendix in Liao (2011*b*).

REFERENCES

ABDOLALI, A. & KIRBY, J. T. 2017 Role of compressibility on tsunami propagation. *J. Geophys. Res. Oceans* **122** (12), 9780–9794.

ARDHUIN, F. & HERBERS, T. H. C. 2013 Noise generation in the solid earth, oceans and atmosphere, from nonlinear interacting surface gravity waves in finite depth. *J. Fluid Mech.* **716**, 316–348.

ARDHUIN, F., LAVANANT, T., OBREBSKI, M., MARIE, L., ROYER, J.-Y., D'EU, J.-F., HOWE, B. M., LUKAS, R. & AUCAN, J. 2013 A numerical model for ocean ultra-low frequency noise: wave-generated acoustic-gravity and Rayleigh modes. *J. Acoust. Soc. Am.* **134** (4), 3242–3259.

BENNEY, D. J. 1962 Non-linear gravity wave interations. *J. Fluid Mech.* **14** (4), 577–584.

BOWEN, S. P., RICHARD, J. C., MANCINI, J. D., FESSATIDIS, V. & CROOKER, B. 2003 Microseism and infrasound generation by cyclones. *J. Acoust. Soc. Am.* **113** (5), 2562–2573.

BRETHERTON, F. P. 1964 Resonant interactions between waves. The case of discrete oscillations. *J. Fluid Mech.* **20** (3), 457–479.

DALRYMPLE, R. A. & ROGERS, B. D. 2006 A note on wave celerities on a compressible fluid. In *Proceedings of the 30th International Conference on Coastal Engineering*, pp. 3–13.

DIAS, F. & BRIDGES, T. J. 2006 The numerical computation of freely propagating time-dependent irrotational water waves. *Fluid Dyn. Res.* **38**, 803–830.

DYACHENKO, A. & ZAKHAROV, V. 1994 Is free-surface hydrodynamics an integrable system? *Phys. Lett.* A **190** (2), 144–148.

EYOV, E., KLAR, A., KADRI, U. & STIASSNIE, M. 2013 Progressive waves in a compressible-ocean with an elastic bottom. *Wave Motion* **50**, 929–939.

FARRELL, W. E. & MUNK, W. 2010 Booms and busts in the deep. *J. Phys. Oceanogr.* **40** (9), 2159–2169.

KADRI, U. 2015 Wave motion in a heavy compressible fluid: revisited. *Eur. J. Mech.* (B/*Fluids*) **49**, 50–57.

KADRI, U. 2017 Tsunami mitigation by resonant triad interaction with acoustic-gravity waves. *Heliyon* **3**, e00234.

KADRI, U. & AKYLAS, T. R. 2016 On resonant triad interactions of acoustic-gravity waves. *J. Fluid Mech.* **788**, R1.

KADRI, U. & STIASSNIE, M. 2012 Acoustic-gravity waves interacting with the shelf break. *J. Geophys. Res.* **117**, C03035.

KADRI, U. & STIASSNIE, M. 2013 Generation of an acoustic-gravity wave by two gravity waves, and their subsequent mutual interaction. *J. Fluid Mech.* **735**, R6.

KIBBLEWHITE, A. C. & EWANS, K. C. 1985 Wave–wave interactions, microseisms, and infrasonic ambient noise in the ocean. *J. Acoust. Soc. Am.* **78** (3), 981–994.

KIBBLEWHITE, A. C. & WU, C. Y. 1991 The theoretical description of wave–wave interactions as a noise source in the ocean. *J. Acoust. Soc. Am.* **89** (5), 2241–2252.

LIAO, S. J. 1992 Proposed homotopy analysis techniques for the solution of nonlinear problem. PhD thesis, Shanghai Jiao Tong University.

LIAO, S. J. 2003 *Beyond Perturbation: Introduction to the Homotopy Analysis Method*. Chapman & Hall/CRC.

LIAO, S. J. 2010 An optimal homotopy-analysis approach for strongly nonlinear differential equations. *Commun. Nonlinear Sci. Numer. Simul.* **15** (8), 2003–2016.

LIAO, S. J. 2011*a* *Homotopy Analysis Method in Nonlinear Differential Equations*. Springer.

LIAO, S. J. 2011*b* On the homotopy multiple-variable method and its applications in the interactions of nonlinear gravity waves. *Commun. Nonlinear Sci. Numer. Simul.* **16** (3), 1274–1303.

LIAO, S. J., XU, D. L. & STIASSNIE, M. 2016 On the steady-state nearly resonant waves. *J. Fluid Mech.* **794**, 175–199.

LIU, Z. & LIAO, S. J. 2014 Steady-state resonance of multiple wave interactions in deep water. *J. Fluid Mech.* **742**, 664–700.

LIU, Z., XU, D. L., LI, J., PENG, T., ALSAEDI, A. & LIAO, S. J. 2015 On the existence of steady-state resonant waves in experiments. *J. Fluid Mech.* **763**, 1–23.

LIU, Z., XU, D. L. & LIAO, S. J. 2018 Finite amplitude steady-state wave groups with multiple near resonances in deep water. *J. Fluid Mech.* **835**, 624–653.

LONGUET-HIGGINS, M. S. 1950 A theory of the origin of microseisms. *Phil. Trans. R. Soc. Lond.* A **243** (857), 1–35.

LONGUET-HIGGINS, M. S. 1962 Resonant interactions between two trains of gravity waves. *J. Fluid Mech.* **12** (3), 321–332.

MADSEN, P. A. & FUHRMAN, D. R. 2012 Third-order theory for multi-directional irregular waves. *J. Fluid Mech.* **698**, 304–334.

NAUGOLNIKH, K. A. & RYBAK, S. A. 2003 Sound generation due to the interaction of surface waves. *Acoust. Phys.* **49** (1), 88–90.

OLIVEIRA, T. C. A. & KADRI, U. 2016 Pressure field induced in the water column by acoustic–gravity waves generated from sea bottom motion. *J. Geophys. Res. Oceans* **121** (10), 7795–7803.

PELLET, L., CHRISTODOULIDES, P., DONNE, S., BEAN, C. J. & DIAS, F. 2017 Pressure induced by the interaction of water waves with nearly equal frequencies and nearly opposite directions. *Theor. Appl. Mech. Lett.* **7** (3), 138–144.

PHILLIPS, O. M. 1960 On the dynamics of unsteady gravity waves of finite amplitude. *J. Fluid Mech.* **9** (2), 193–217.

RENZI, E. & DIAS, F. 2014 Hydro-acoustic precursors of gravity waves generated by surface pressure disturbances localised in space and time. *J. Fluid Mech.* **754**, 250–262.

STIASSNIE, M. 2010 Tsunamis and acoustic-gravity waves from underwater earthquakes. *J. Engng Maths* **67**, 23–32.

VAJRAVELU, K. & VAN GORDER, R. A. 2012 *Nonlinear Flow Phenomena and Homotopy Analysis: Fluid Flow and Heat Transfer*. Springer.

VAN GORDER, R. A. & VAJRAVELU, K. 2008 Analytic and numerical solutions to the Lane–Emden equation. *Phys. Lett.* A **372** (39), 6060–6065.

WEBB, S. C. 1992 The equilibrium oceanic microseism spectrum. *J. Acoust. Soc. Am.* **92** (4), 2141–2158.

WEBB, S. C. 1998 Broadband seismology and noise under the ocean. *Rev. Geophys.* **36** (1), 105–142.

XU, D. L., LIN, Z. L., LIAO, S. J. & STIASSNIE, M. 2012 On the steady-state fully resonant progressive waves in water of finite depth. *J. Fluid Mech.* **710**, 379–418.

YAMAMOTO, T. 1982 Gravity waves and acoustic waves generated by submarine earthquakes. *Soil Dyn. Earthquake Eng.* **1**, 75–82.

ZHONG, X. X. & LIAO, S. J. 2017 Approximate solutions of Von Kármán plate under uniform pressure-equations in differential form. *Stud. Appl. Maths* **138** (4), 371–400.

ZHONG, X. X. & LIAO, S. J. 2018*a* Analytic approximations of Von Kármán plate under arbitrary uniform pressure-equations in integral form. *Sci. China Phys. Mech. Astronom.* **61**, 014611.

ZHONG, X. X. & LIAO, S. J. 2018*b* On the limiting Stokes wave of extreme height in arbitrary water depth. *J. Fluid Mech.* **843**, 653–679.